

USE OF A GAS JET TECHNIQUE TO PREPARE MICROCRYSTALLINE SILICON BASED SOLAR CELLS AT HIGH I-LAYER DEPOSITION RATES

S.J. Jones, R. Crucet, X. Deng, J. Doehler, R. Kopf, A. Myatt, D.V. Tsu and M. Izu,
Energy Conversion Devices, Inc., Troy, MI 48084

ABSTRACT

Using a Gas Jet thin film deposition technique, microcrystalline silicon ($\mu\text{-Si}$) materials were prepared at rates as high as 15-20 $\text{\AA}/\text{s}$. The technique involves the use of a gas jet flow that is subjected to a high intensity microwave source. The quality of the material has been optimized through the variation of a number of deposition conditions including the substrate temperature, the gas flows, and the applied microwave power. The best films were made using deposition rates near 16 $\text{\AA}/\text{s}$. These materials have been used as i-layers for red light absorbing, nip single-junction solar cells. Using a 610nm cutoff filter which only allows red light to strike the device, pre-light soaked currents as high as 10 mA/cm^2 and 2.2-2.3% red-light pre-light soaked peak power outputs have been obtained for cells with i-layer thicknesses near 1 micron. This compares with currents of 10-11 mA/cm^2 and 4% initial red-light peak power outputs obtained for high efficiency amorphous silicon germanium alloy (a-SiGe:H) devices. The AM1.5 white light efficiencies for these microcrystalline cells are 5.9-6.0%. While the efficiencies for the a-SiGe:H cells degrade by 15-20% after long term light exposure, the efficiencies for the microcrystalline cells before and after prolonged light exposure are similar, within measurement error. Considering these results, the Gas Jet deposition method is a promising technique for the deposition of $\mu\text{-Si}$ solar cells due to the ability to achieve reasonable stable efficiencies for cells at i-layer deposition rates (16 $\text{\AA}/\text{s}$) which make large-scale production economically feasible.

INTRODUCTION

The poor performance of red light absorbing a-SiGe:H cells as compared with the blue-green light absorbing a-Si:H cells has been widely documented[1]. Larger defect densities, weaker hydrogen bonds and heterogeneous microstructures have all been attributed to the poorer performance for the alloy material. With a-SiGe:H alloys commonly used as red light absorbing i-layers for the component cells of high stable efficiency triple-junction devices, the poorer performance limits the achievable efficiencies for the triple-junction modules presently made in production. In addition, the cost of germane gas presently used to make the alloy material is a significant expense in the manufacturing process while silane gas is a low material cost item. Thus, it would be desirable in terms of both stable cell efficiency and module cost to find an alternative low bandgap, red light absorbing material to replace a-SiGe:H as i-layers for bottom cells of the triple-junction structure.

One possible alternative material is microcrystalline Si ($\mu\text{-Si}$), which has a bandgap near 1.1 eV. Shah et. al.[2] have shown that high quality $\mu\text{-Si}$ pin devices with 8.5% efficiencies that absorb a significant amount of the red light and do not degrade with long term light exposure can be made using the Very High Frequency PECVD technique (VHF). However in using this or any standard PECVD technique, the deposition rates of the $\mu\text{-Si}$ materials are limited to 1-5 $\text{\AA}/\text{s}$. Because the $\mu\text{-Si}$ i-layers must be nearly 1 micron thick due to their low light absorption efficiencies as compared with the amorphous materials (amorphous i-layers are typically 1000-2000 \AA thick), the low deposition rates make the use of the PECVD techniques economically unsound for the large scale production of microcrystalline materials and solar cells.

Here we report results for $\mu\text{-Si}$ materials and nip cells made using a new Gas Jet technique[3]. This technique, in which high speed gas is subjected to high intensity microwaves, allows for the preparation of these microcrystalline materials at rates as high as 15-20 $\text{\AA}/\text{s}$.

EXPERIMENT

The $\mu\text{-Si}$ materials were prepared in a single chamber system whose vacuum was maintained using a diffusion pump. A microwave source with a fixed 2.54 GHz frequency was used to dissociate the feed gases that included silane, hydrogen and various fluorine-based etching gases. To optimize the material properties, the following parameters were systematically varied; substrate temperature, active gas flows, hydrogen dilution, and the applied microwave power.

To fabricate nip solar cell structures, doped layers were prepared using the standard PECVD process and deposition rates near 1 $\text{\AA}/\text{s}$. Also, current enhancing Ag/ZnO back reflectors were deposited on the stainless steel substrates prior to fabrication of the nip semiconductor structures. The back reflectors were prepared using a DC sputtering technique. Because of equipment limitations, the doped layers were prepared in a separate deposition system so that the n/i and i/p interfaces were exposed to the atmosphere and are likely oxidized. The authors recognize that this oxidation could limit our cell efficiencies. After fabrication of the nip structure, the devices were completed by depositing Indium Tin Oxide (ITO) conductive layers and then Al collection grids. Both the ITO and Al layers were prepared using standard evaporation techniques.

To characterize the cells, standard current vs. voltage (IV) and spectral response (quantum efficiency) measurements were made. Since our goal is to use the microcrystalline cells as the red light absorbing components of multi-junction cells, IV measurements were completed using not only the direct AM1.5 white light but also the white light filtered with a 610 nm low band pass filter to simulate the absorption due to higher bandgap, blue-green light absorbing top layers. To complete light soaking studies, the cells were subjected to 400-1400 hrs. of one sun light with the cell temperature fixed at 50°C. The i-layer thicknesses were determined using standard capacitance techniques.

To classify the microcrystalline film microstructure, Infrared Absorption Spectroscopy and Raman Spectroscopy measurements were completed to characterize the structural bonding in the films and the degree of microcrystallinity. Also photoconductivity and dark conductivity measurements were completed using AM1.5 light intensities.

RESULTS

Material Properties

Figure 1 displays photocurrent-to-dark current (photo/dark) ratios for Gas Jet single layer films deposited on 7059 glass and prepared with different silane (SiH_4) gas flows. All other deposition conditions were nominally fixed for this set of samples. With the SiH_4 flow decreasing from 30 to 20 sccm there is a sudden drop in the photo/dark ratio indicative of a change in film microstructure. The drop is almost exclusively due to an increase in the dark conductivity which is indicative of the growth of microcrystals in the previously amorphous film. Figure 2 displays Raman data for two of these films made using SiH_4 flows of 20 and 40 sccm. The sharp peaks near 530 and 560 cm^{-1} are Ar Laser lines and are not related to the measured film microstructure. The presence of the peak near 520 cm^{-1} is related to Si microcrystals. The fact that this peak is present in the spectra for the film made with $\text{SiH}_4=20$ sccm and not in the spectra for the $\text{SiH}_4=40$ film demonstrates that the change in the electrical properties with SiH_4 flow is related to an amorphous Silicon-to-microcrystalline Si transition.

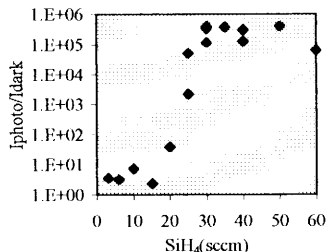


Figure 1. Photo-to-dark current values for films made using different SiH₄ flows.

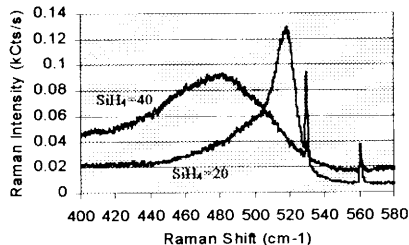


Figure 2. Raman Spectra for films made using different SiH₄ flows.

Figure 3 compares Photothermal Deflection Spectroscopy (PDS) data for films made using SiH₄ flows of 15 and 40 sccm. The enhanced absorption at lower energies for the film made with the lower SiH₄ flow is again consistent with a lower bandgap, red-light absorbing microcrystalline silicon film. Figure 4 demonstrates that as the material becomes $\mu\text{-Si}$ with the lower SiH₄ flow, the deposition rates decreases. However, when a SiH₄ flow between 15 and 25 sccm is used, the films are microcrystalline and deposition rates between 10 and 20 $\text{\AA}/\text{s}$ are obtained. The degree of microcrystallinity can further be enhanced while maintaining high rates through proper selection of hydrogen dilution, gas flows and applied microwave power.

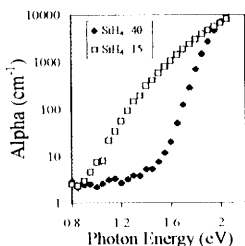


Figure 3. PDS Spectra for films made using different SiH₄ flows.

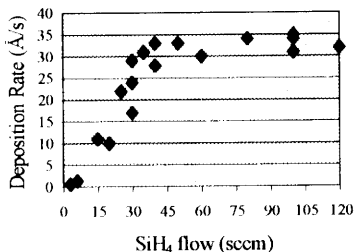


Figure 4. Deposition rates for films made using different SiH₄ flows.

Cells Properties

The nip cells with $\mu\text{-Si}$ i-layers were fabricated using the procedures outlined in the experimental section. The i-layer thicknesses were between 0.8 and 1.1 microns with an average deposition rate of 16 $\text{\AA}/\text{s}$. This made the average i-layer preparation time equal to 10.5 min. Figure 5 compares a spectral response curve for a $\mu\text{-Si}$ device with high quality a-Si:H and a-SiGe:H solar cells. Both of the amorphous i-layers were prepared using the standard PECVD technique and rates near 1 $\text{\AA}/\text{s}$. The a-Si:H i-layer is much thicker than what is typically used in a triple-junction device while the a-SiGe:H device is representative of a bottom component cell. From the figure, it is clear that the $\mu\text{-Si}$ cell absorbs a significant amount of red light in the 750-950 nm region of the spectrum, light not collected by the a-Si:H device. Compared with the a-SiGe:H device, the present microcrystalline devices do not absorb as much total red light as the alloy cells do, however they do absorb more light above 900 nm due to their lower bandgap.

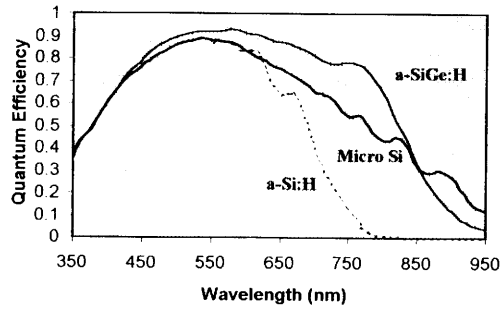


Figure 5. Comparison of quantum efficiency curves for a-Si:H, a-SiGe:H and μ c-Si cells.

Table I displays data from IV measurements of some of these microcrystalline devices made in the early part of the program. This IV data was obtained using AM1.5 light that was filtered using a 610nm low bandpass filter. Again, use of this red light truly tests the potential use of the cell as a red-light absorbing bottom cell in a multi-junction solar cell structure. Under these conditions, the microcrystalline cells typically have V_{oc} values of 0.42-0.43 V, J_{sc} values between 8.5 and 10 mA/cm^2 (21-23 mA/cm^2 under white light conditions) and FF of 0.47-0.53. These data can be compared with those listed in the same table for a high quality a-SiGe:H cell typically used as a bottom cell for a triple-junction a-Si:H/a-Si(Ge):H/a-SiGe:H solar cell. This cell was prepared at United Solar using the standard PECVD technique and an i-layer deposition rate near 1 $\text{\AA}/\text{s}$. From the data it is clear that the a-SiGe:H cells are superior, particularly in terms of pre-light soaked V_{oc} and FF. The smaller V_{oc} for the microcrystalline cells is mostly due to the

Table I
Light soaking completed using unfiltered white light.
IV data taken using AM1.5 light filtered with 610nm cutoff filter (red light).

Cells	Light Soak Time(hr.)	V_{oc} (V)	J_{sc} (mA/cm^2)	FF	R_s (ohmcm^2)	P_{max} (mW/cm^2)	Q.E. 700 nm	Q.E. 900 nm
Gas Jet μ c-Si cell 1	0	0.421	9.4	0.523	9.4	2.02	0.63	0.21
	170	0.410	9.3	0.530	9.2	2.01	-	-
	1100	0.412	9.1	0.524	9.6	1.97	-	-
Gas Jet μ c-Si cell 2	0	0.420	10.0	0.469	10.5	1.96	0.68	0.22
	170	0.418	9.8	0.472	10.8	1.92	-	-
	1100	0.419	9.7	0.460	12.1	1.87	-	-
Gas Jet μ c-Si cell 3	0	0.429	9.1	0.485	11.8	1.89	0.72	0.20
	500	0.425	9.2	0.474	12.4	1.86	-	-
	1400	0.428	9.1	0.464	13.7	1.80	-	-
Gas Jet μ c-Si cell 4	0	0.428	8.4	0.534	10.9	1.91	0.62	0.19
	500	0.428	8.4	0.526	11.3	1.90	-	-
	1400	0.430	8.3	0.519	12.3	1.84	-	-
Gas Jet μ c-Si cell 5	0	0.426	9.2	0.519	10.1	2.02	-	-
Gas Jet μ c-Si cell 6	0	0.428	8.8	0.530	10.1	2.00	-	-
PECVD a-SiGe:H	0	0.615	10.5	0.595	14.1	3.84	0.81	0.12

smaller bandgap for the material. Some improvements in the V_{oc} should come with optimization of the doped layer deposition conditions. The deposition conditions used for doped layers in these devices were optimized for amorphous Si based i-layers but have yet to be optimized for the microcrystalline i-layers. These cells were light soaked under AM1.5 white light conditions for over 1000 hrs to test their stability. The cell efficiencies degrade by less than 5%, values close to the measurement error. This high degree of stability is consistent with $\mu\text{-Si}$ solar cells and is not found for the amorphous based devices.

Higher red-light peak power output (P_{max}) for the Gas Jet produced microcrystalline cells were obtained when different fluorine-based gases were used in the process. Table II shows IV data for these devices. Higher FF and V_{oc} led to $P_{max}=2.2\text{-}2.3\text{ mW/cm}^2$ and larger currents should be obtained for thicker i-layers. Figures 6 and 7 display IV curves for these cells measured under the standard white light conditions demonstrating 5.9-6.0% efficiencies. Using Raman spectroscopy, it was demonstrated that the use of this fluorine-based gas led to enhanced crystallinity, suggesting that the increase in V_{oc} is not related to an increase in the amorphous tissue but to an improvement in the material and/or the i-layer/doped layer interface quality. These cells were light soaked along with a high quality a-SiGe:H cell to directly compare the stability of the two types of cells. Since we are testing the feasibility of using these cells as bottom cells for the triple-junction structure, the light soaking was completed using white light which was filtered using a low bandpass filter to simulate the light absorbed by the top and middle cells. As can be seen from the data in the table, the P_{max} values for the $\mu\text{-Si}$ devices remain exposure, the P_{max} for the a-SiGe:H cell degrades by 17% demonstrating the enhanced stability for the $\mu\text{-Si}$ cells.

Table II
Light Soaking Conditions: white light filtered with 570nm low band pass filter, 50°C.
IV data taken using AM1.5 light filtered with 610nm cutoff filter (red light).

Cell Type	Light Soak Time (hr.)	V_{oc} (V)	J_{sc} (mA/cm^2)	FF	R_s (ohmcm^2)	P_{max} (mW/cm^2)	% of Degr.
PECVD a-SiGe:H	0	0.615	10.5	0.595	14.1	3.84	-
	1030	0.595	10.3	0.522	24.4	3.18	17.2
Gas Jet $\mu\text{-Si}$ cell 1	0	0.462	8.22	0.584	8.9	2.22	-
	1030	0.467	8.16	0.574	10.2	2.19	1.4
Gas Jet $\mu\text{-Si}$ cell 2	0	0.473	8.52	0.560	9.6	2.26	-
	1030	0.481	8.56	0.550	10.9	2.26	0

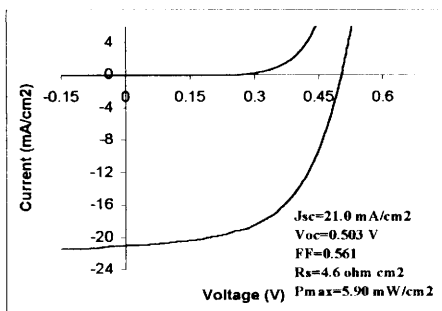


Figure 6. IV plot for $\mu\text{-Si}$ cell.

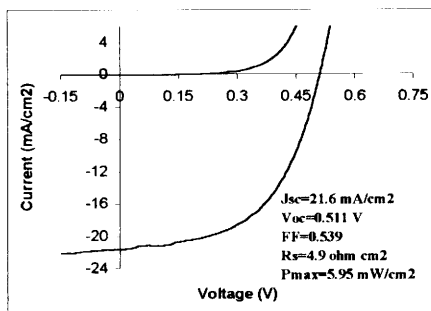


Figure 7. IV plot for $\mu\text{-Si}$ cell.

DISCUSSION AND CONCLUSIONS

The ability to create $\mu\text{-Si}$ material at such high deposition rates with the Gas Jet technique is related to the use of microwaves to achieve high decomposition rates for SiH_4 while still allowing for high flows of hydrogen gas for enhanced etching at the film surface. Similar conditions can be obtained using conventional microwave techniques where high deposition rates for $\mu\text{-Si}$ growth have also been reported[4]. However with the use of the high-speed gas jet with this technique, there is little time for gas reactions after SiH_4 decomposition thus minimizing the chance for polysilane radical formation which may limit material quality and cell performance.

The efficiencies for the cells are respectable however they do not match the 8.5% AM1.5 efficiency for the $\mu\text{-Si}$ cells² made at 1 $\text{\AA}/\text{s}$ using the VHF method nor the light soaked 3.2% red-light efficiency for high quality a-SiGe:H cells (see Table 2). However, expanding the VHF technique to deposition rates of 11 and 14 $\text{\AA}/\text{s}$, only lower efficiencies of 5.2 and 3.6%, respectively, have been achieved[5]. It should be noted that for the cells reported here, both doped/i-layer interfaced were exposed to air prior to subsequent layer deposition, and the doped layer and the back reflector deposition conditions have yet been optimized specifically for the microcrystalline i-layer. In particular, the microcrystalline material has a more textured surface than the typical amorphous silicon i-layers leading to different requirements for the doped layers and the back reflector layers. Further optimization of the different cell layers and preparation of all semiconductor layers in a load-locked system should lead to higher cell performance.

In terms of other techniques with which $\mu\text{-Si}$ can be made at high deposition rates, the Hot Wire technique has been used to make these materials at rates of 15-20 $\text{\AA}/\text{s}$ [6]. However, $\mu\text{-Si}$ cells made using this technique have, to the author's knowledge, yet to achieve AM1.5 white light efficiencies above 4%. However, both the Hot wire and the Gas Jet techniques are in their infant stages in terms of their use for making $\mu\text{-Si}$ devices and thus further studies are needed to fully assess their potential application in making high rate $\mu\text{-Si}$ i-layers for solar cells.

In conclusion, it has been demonstrated that the Gas Jet technique can be used to prepare $\mu\text{-Si}$ i-layers for nip solar cell devices at rates of 16 $\text{\AA}/\text{s}$. The cells have 2.2% red-light P_{max} (6.0% white-light) that remain stable with long term light exposure. With improvement of the cell performance, this process could be applicable for use in the production of large-area modules with high stable efficiencies due to the ability to make the microcrystalline materials at high deposition rates.

ACKNOWLEDGEMENTS

We would like to thank A. Banerjee, J. Noch, N. Jackett, J. Edens and T. Palmer of United Solar and B. Viers of ECD for their efforts in preparation of doped layers and ITO contacts. This work was partially funded by the Department of Energy under the Grant No. DE-FG02-96ER82162 and by the National Science Foundation under the Award No. DMI-9760805.

REFERENCES

1. For review, W. Luft, Proc. of 20th IEEE Photovoltaics Spec. Conf. 218 (1988).
2. J. Meier, H. Keppner, S. Dubail, U. Kroll, P. Torres, P. Pernet, Y. Ziegler, J.A. Anna Selvan, J. Cuperus, D. Fischer, A. Shah, Mat. Res. Soc. Symp. Proc. 507, 139 (1998).
3. J. Doehler, S. Hudgens, S.R. Ovshinsky, B. Dotter, L. R. Peedin, J.M. Krisko, A. Krisko, United States Patents #4,883,686 and 5,093,149 (1988).
4. J.Schellenberg, R. Mcleod, S. Mejia, H. Card, K. Kao, Appl. Phys. Lett., 48(2), 163 (1986).
5. P.Torres,J.Meier,U.Kroll, N.Beck, H.Keppner, A.Shah, 26th IEEE Photo. Sp. Con.,711(1997).
6. J. Rath, A. van Zutphen, H. Meiling, R. Schropp, Mat. Res. Soc. Proc. 467, 445 (1997).